

# Source Driven Free Boundary Modes

Eugene Y. Chen  
H. L. Berk  
Boris Breizman  
L.-J. Zheng

IFS, UT Austin

# Outline

- The AEGIS formalism
- Free Boundary TAE
- The source inversion code
- Driven modes – benchmark near eigenfrequency
- Second Harmonics of C-Mod TAE
- Conclusions

# The AEGIS Formalism (1)

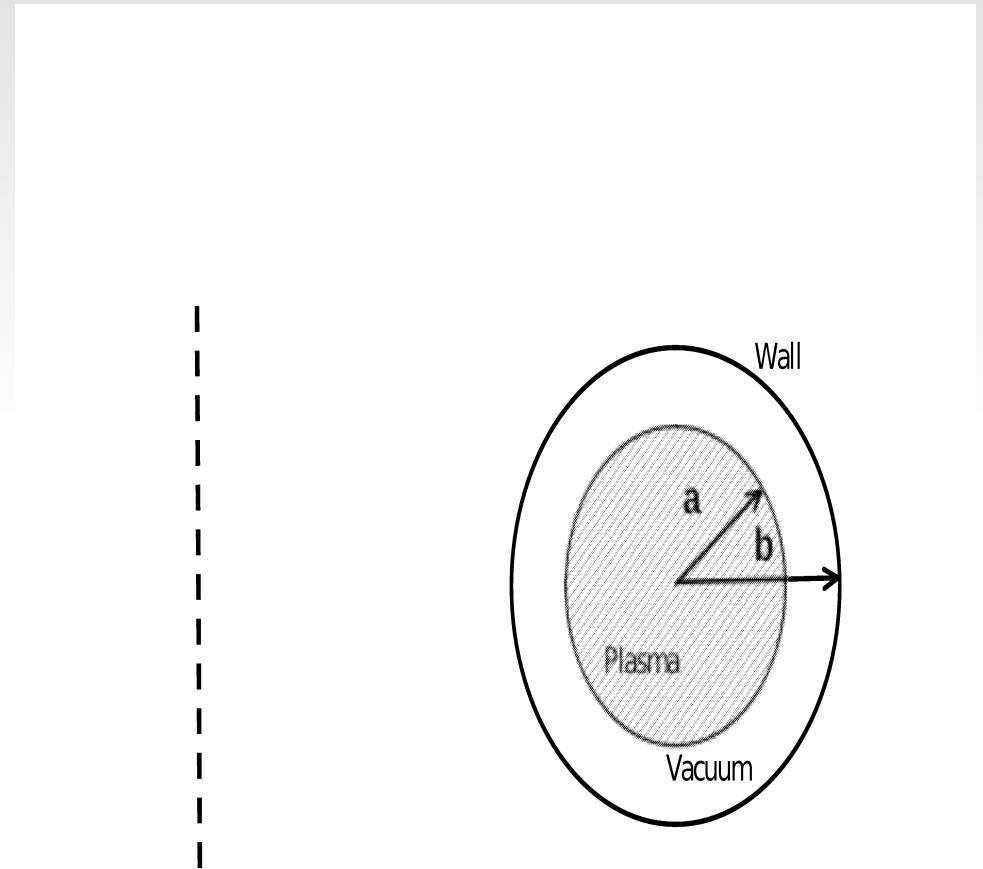
- AEGIS is an ideal MHD eigenvalue code.
- It solves the *magnetic displacement* inside a toroidal plasma:
- $$(\mathcal{F}\tilde{\xi}^{\psi'} + \mathcal{K}\tilde{\xi}^{\psi})' - \mathcal{K}^{\dagger}\tilde{\xi}^{\psi'} - \mathcal{G}\tilde{\xi}^{\psi} = 0$$
- It assumes the toroidal plasma is surrounded by a vacuum region, enclosed by a perfectly conducting wall.

# The AEGIS formalism (2)

- In the vacuum region, magnetic scalar potential is solved:

$$\nabla^2 u = 0$$

- AEGIS matches the plasma solution and the vacuum solution at the plasma–vacuum interface.



# The AEGIS formalism (3)

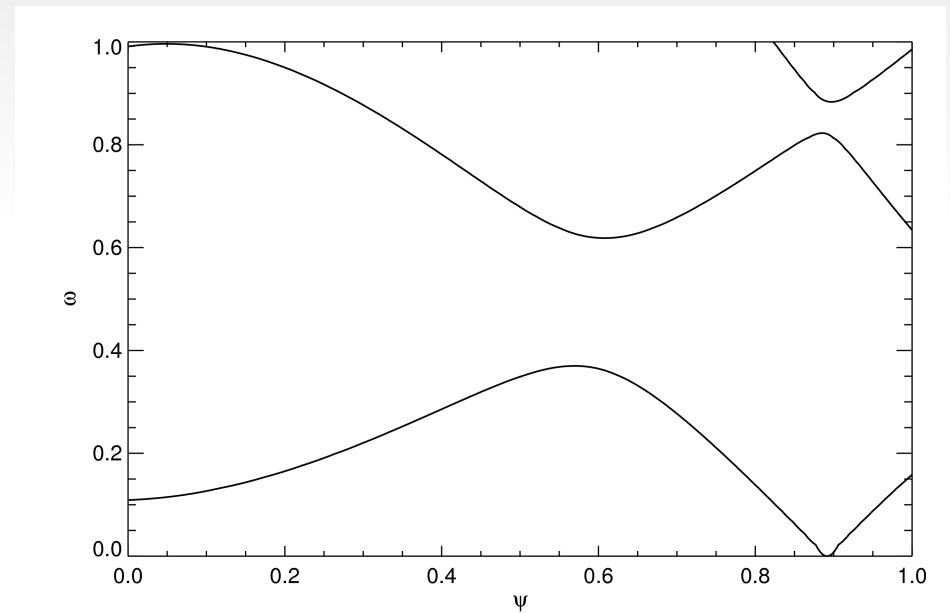
- The process can be divided into two steps. (i) solving independent solutions in each region. (ii) solve for the linear combination for an exact match – this poses an eigenvalue problem:

$$\mathbf{L}\hat{\phi} = 0$$

- The matrix  $\mathbf{L}$  contains the boundary values of the  $M$  (total # of poloidal harmonics) independent plasma homogeneous solutions and the matching conditions.

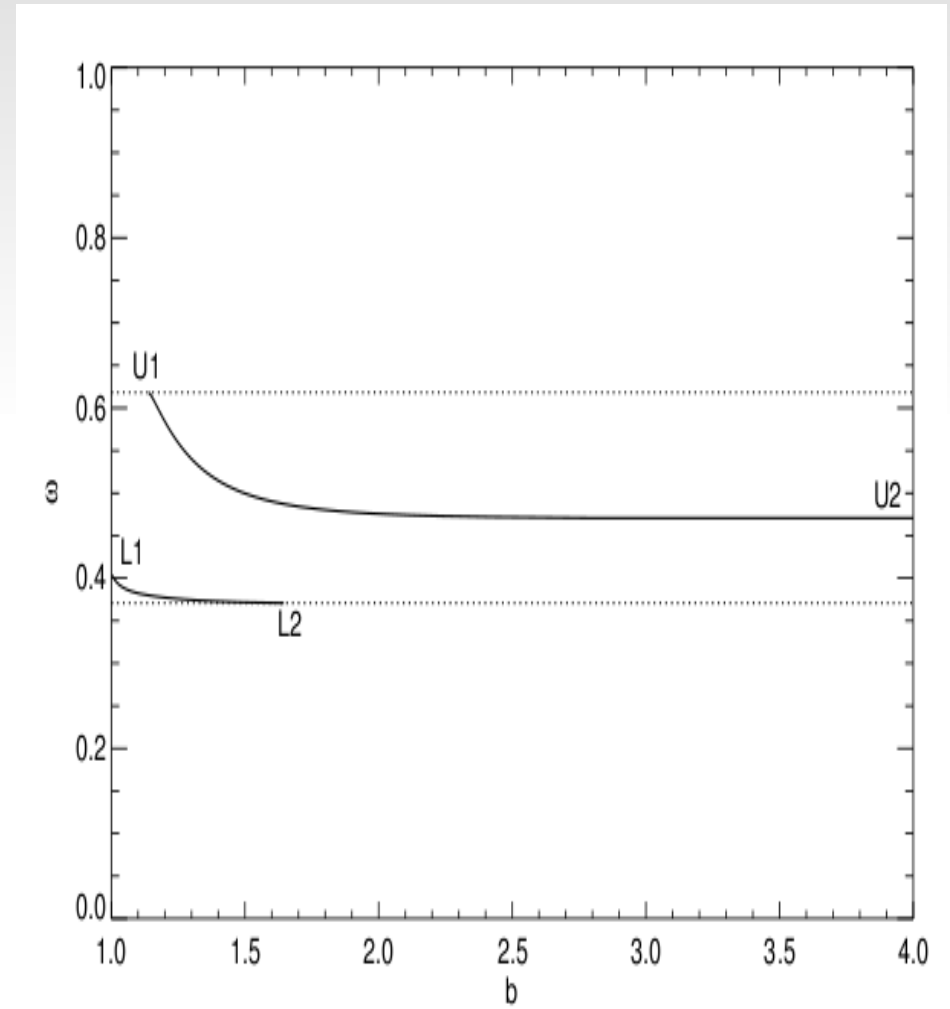
# Application: Free Boundary TAE

- We made parametric study of TAE in free-boundary setting.
- Wall position and other equilibrium parameters are taken as input.
- We consider an equilibrium with a single TAE gap.

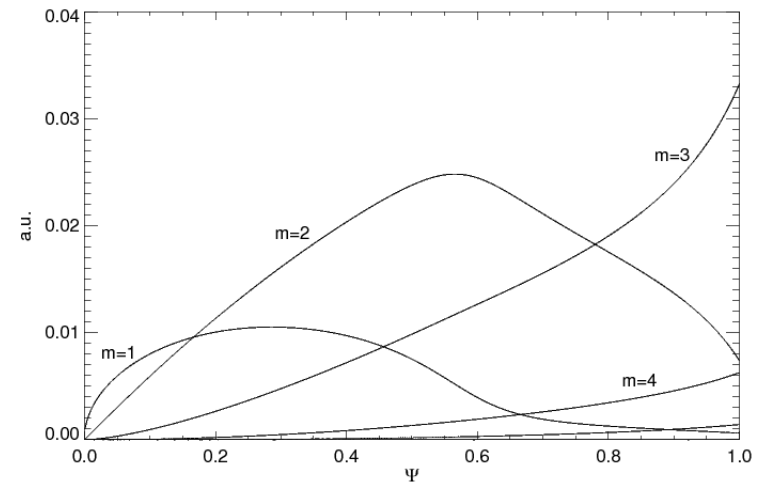
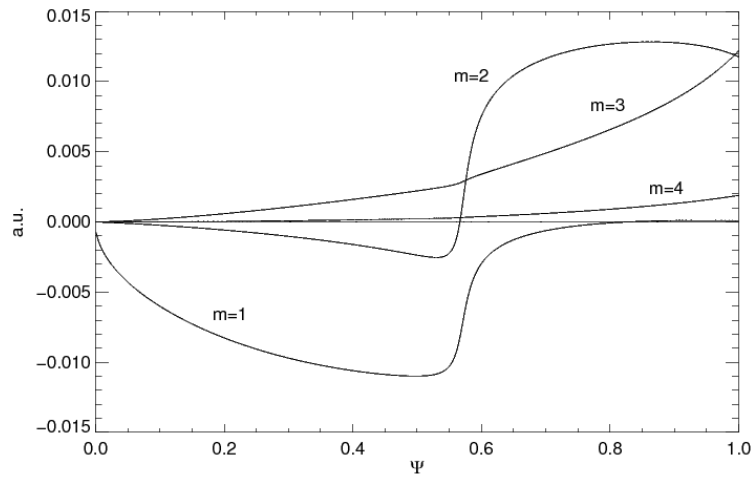
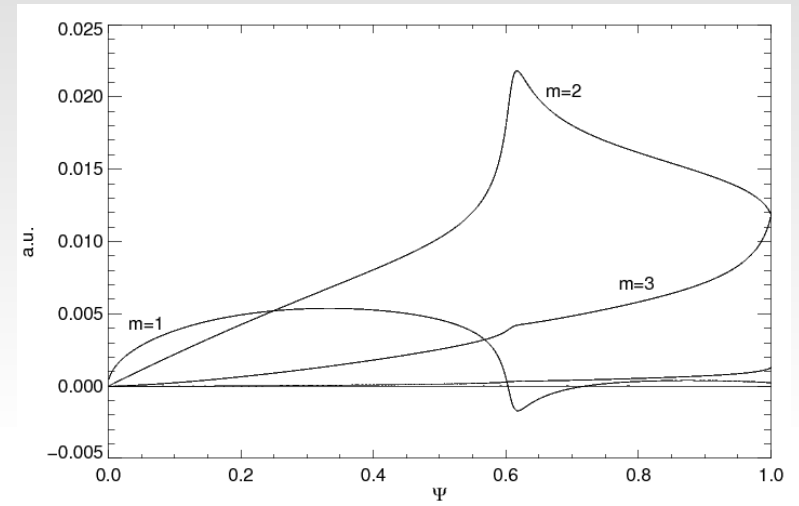
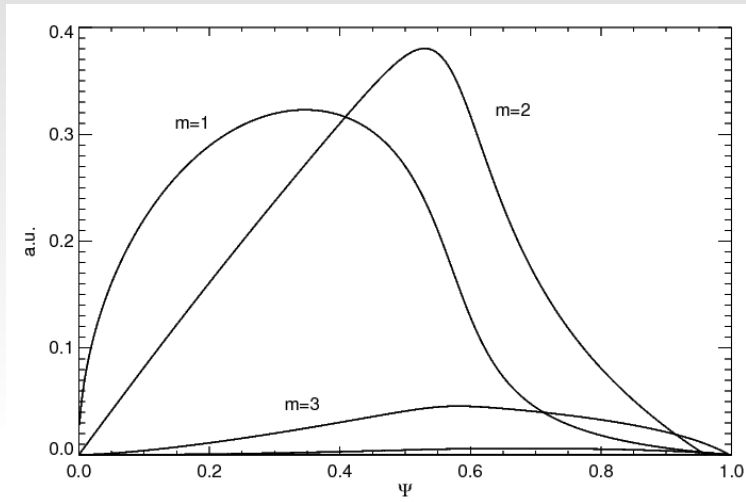


# Wall-Frequency Relation

- The frequency of eigenmode decreases with increasing distance of wall from plasma boundary.
- A new branch of TAE appears *only* with finite wall distance. In this particular equilibrium, the critical distance is  $0.14 a$ .



# Mode Structure



# The Source Inversion Code

- AEGIS was upgraded to deal with plasma driven by a source term.

$$(\mathcal{F}\tilde{\xi}^{\psi'} + \mathcal{K}\tilde{\xi}^{\psi})' - \mathcal{K}^\dagger\tilde{\xi}^{\psi'} - \mathcal{G}\tilde{\xi}^{\psi} = S$$

- A particular solution that has zero magnetic displacement at the plasma–vacuum interface is solved. We record the force exerted by the particular solution as  $\mathbf{u}_2^p$
- It can be shown that the solution which satisfies all the boundary conditions can be found by solving the matrix equation:

$$\mathbf{L}\hat{\phi} + \mathbf{u}_2^p = 0$$

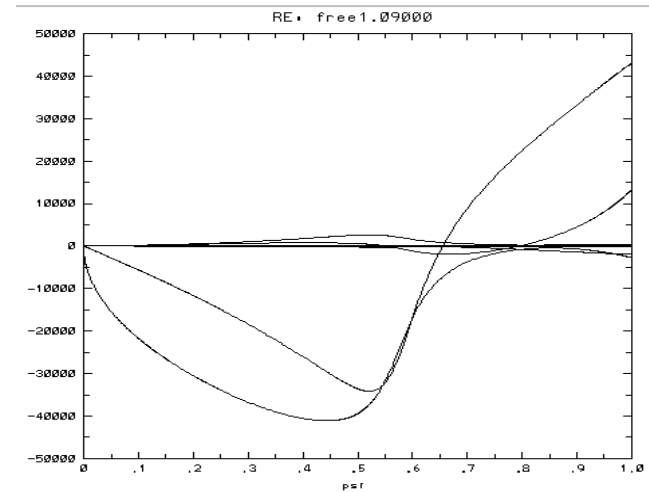
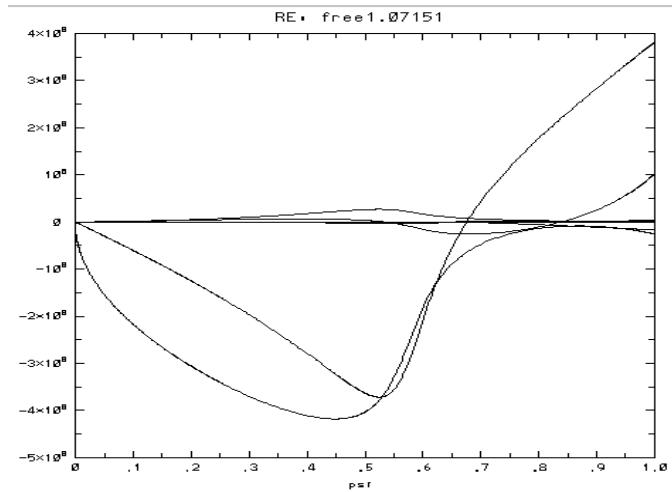
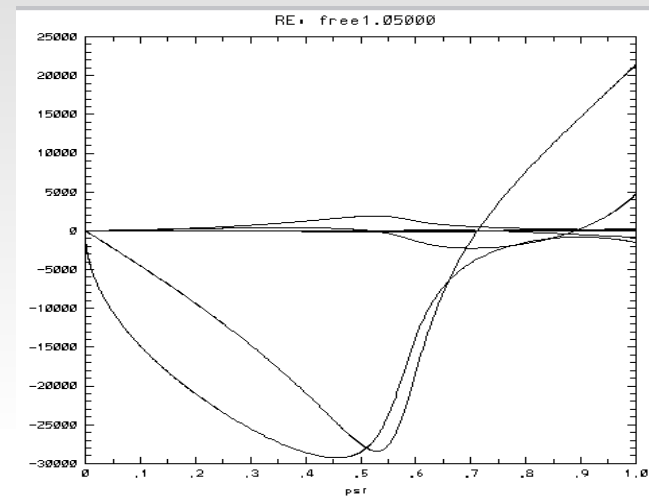
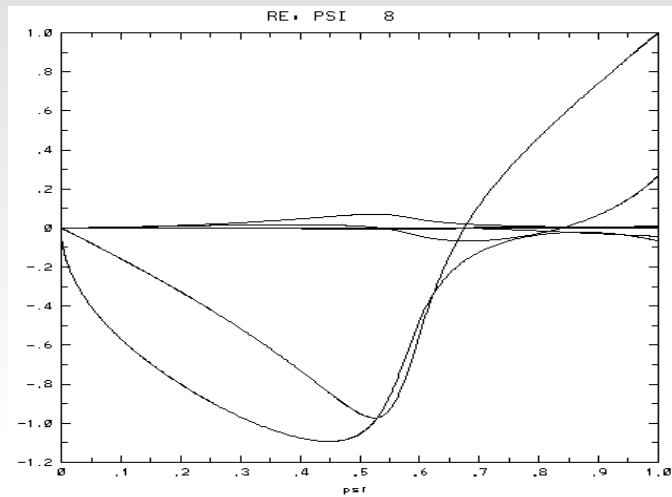
# Driving the plasma with varying vacuum gap size (1)

- We prepare a test driving source for the purpose of illustration:

$$S = \sin(\pi\psi) e^{i(\theta - \phi + \omega_0 t)}$$

- We chose  $\omega_0$  to be  $0.385 V_{A0}/R$ .
- It is the eigen frequency of the lower branch TAE provided  $b/a=1.07$  .

# Driving the plasma with varying vacuum gap size (2)

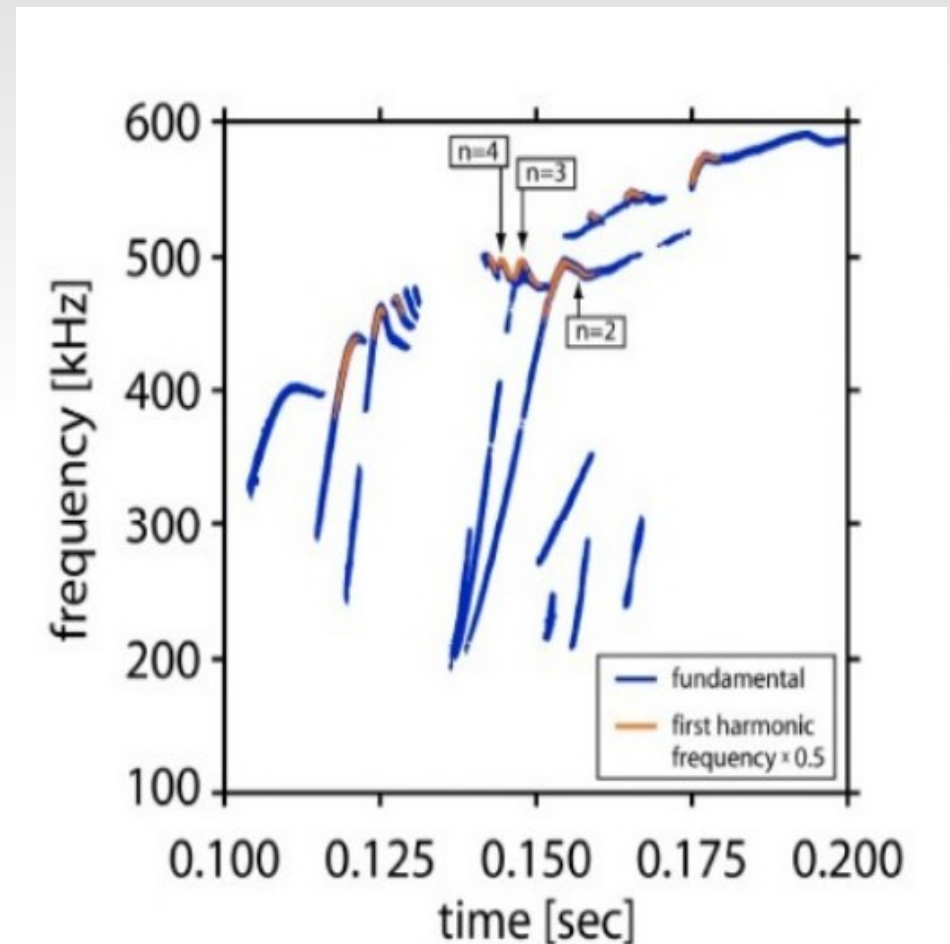


# Driving the plasma with varying vacuum size (3)

- The shape of the mode is found to be similar to the eigenmode instead of the driving source if the driving frequency is close to the eigenfrequency.
- Resonance is observed as vacuum gap size varies.

# Application: 2<sup>nd</sup> harmonics in C-Mod TAE

- 2<sup>nd</sup> harmonics of AE is observed in Alcator C-Mod. Its structure can be compared with PCI measurements (Edlund et al. 2009)
- With the upgraded version of AEGIS, we are able to calculate this structure numerically.



# Numerical Scheme (1)

- The 2<sup>nd</sup> harmonics is needed to fully balance the un-linearized momentum equation.
- On the other hand, we only have a linear MHD solver which ignores the convective derivative term (and consequently, the 2<sup>nd</sup> harmonics).
- However, 2<sup>nd</sup> harmonics can be restored by treating a few quantities derived from the fundamental mode as a driving source.

# Numerical Scheme (2)

- (Smith et al. 2006)

$$4\pi\rho_0\ddot{\mathbf{v}}_1 - (\nabla \times \mathbf{B}_0) \times \nabla \times (\mathbf{v}_1 \times \mathbf{B}_0) \\ - [\nabla \times \nabla \times (\mathbf{v}_1 \times \mathbf{B}_0)] \times \mathbf{B}_0 = 0,$$

$$4\pi\rho_0\ddot{\mathbf{v}}_2 - (\nabla \times \mathbf{B}_0) \times \nabla \times (\mathbf{v}_2 \times \mathbf{B}_0) \\ - [\nabla \times \nabla \times (\mathbf{v}_2 \times \mathbf{B}_0)] \times \mathbf{B}_0 \\ = (\nabla \times \mathbf{B}_0) \times \nabla \times (\mathbf{v}_1 \times \mathbf{B}_1) + [\nabla \times \nabla \times (\mathbf{v}_1 \times \mathbf{B}_1)] \\ \times \mathbf{B}_0 + \frac{\partial}{\partial t} \left[ -4\pi\rho_0(\mathbf{v}_1 \cdot \nabla)\mathbf{v}_1 + (\mathbf{B}_1 \cdot \nabla)\mathbf{B}_1 - 4\pi\rho_1\dot{\mathbf{v}}_1 \right. \\ \left. - \frac{1}{2} \nabla (\mathbf{B}_1 \cdot \mathbf{B}_1) \right],$$

# Numerical Scheme (3)

- As the quantities we calculate depend on the coordinate used. Extra care needs to be taken: e.g.,

$$\vec{v} \equiv e^{-in\zeta} (v_1(\psi, \theta) J \nabla \theta \times \nabla \zeta + v_2(\psi, \theta) J \nabla \zeta \times \nabla \psi + v_3(\psi, \theta) J \nabla \psi \times \nabla \theta)$$

$$v_j(\psi, \theta) = \sum_{m=m_{\min}}^{m_{\max}} \frac{1}{\sqrt{2\pi}} v_{jm}(\psi) e^{im\theta}$$

$$(\vec{v} \cdot \nabla) \vec{v} = \frac{1}{2} e^{-2in\zeta} (4i\mathbf{M}G_{13}v_2v_3 - 2inG_{13}v_3^2 + v_1^2G'_{11} - v_2^2G'_{22} - 2v_2v_3G'_{23} - v_3^2G'_{33}$$

$$+ 2G_{11}v_1(2i\mathbf{M}v_2 - inv_3 + v'_1) + 2G_{12}(iv_2(2\mathbf{M}v_2 - nv_3) + v_1v'_2) + 2G_{13}v_1v'_3) \nabla \psi$$

$$- \frac{1}{2} i e^{-2in\zeta} (\mathbf{M}G_{11}v_1^2 - 3\mathbf{M}G_{22}v_2^2 + 2\mathbf{M}G_{13}v_1v_3 + 2nG_{22}v_2v_3 - 2\mathbf{M}G_{23}v_2v_3$$

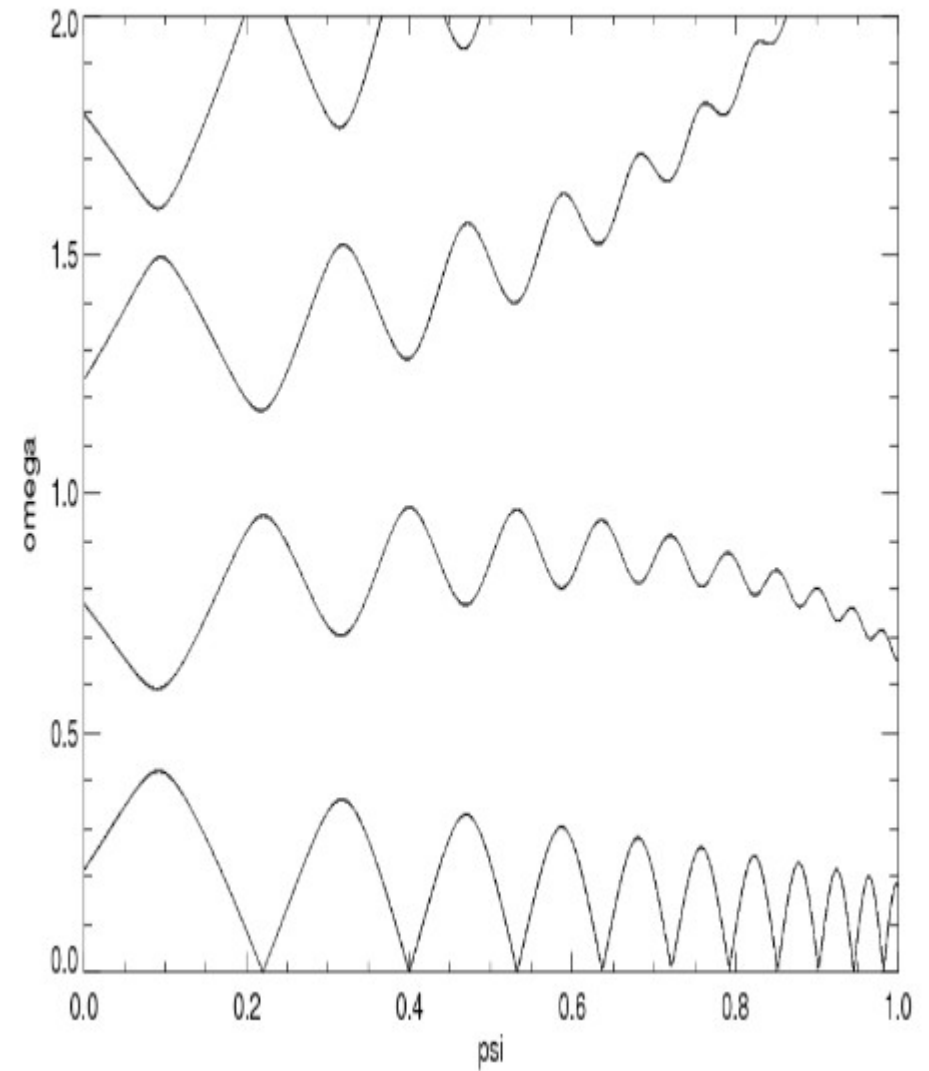
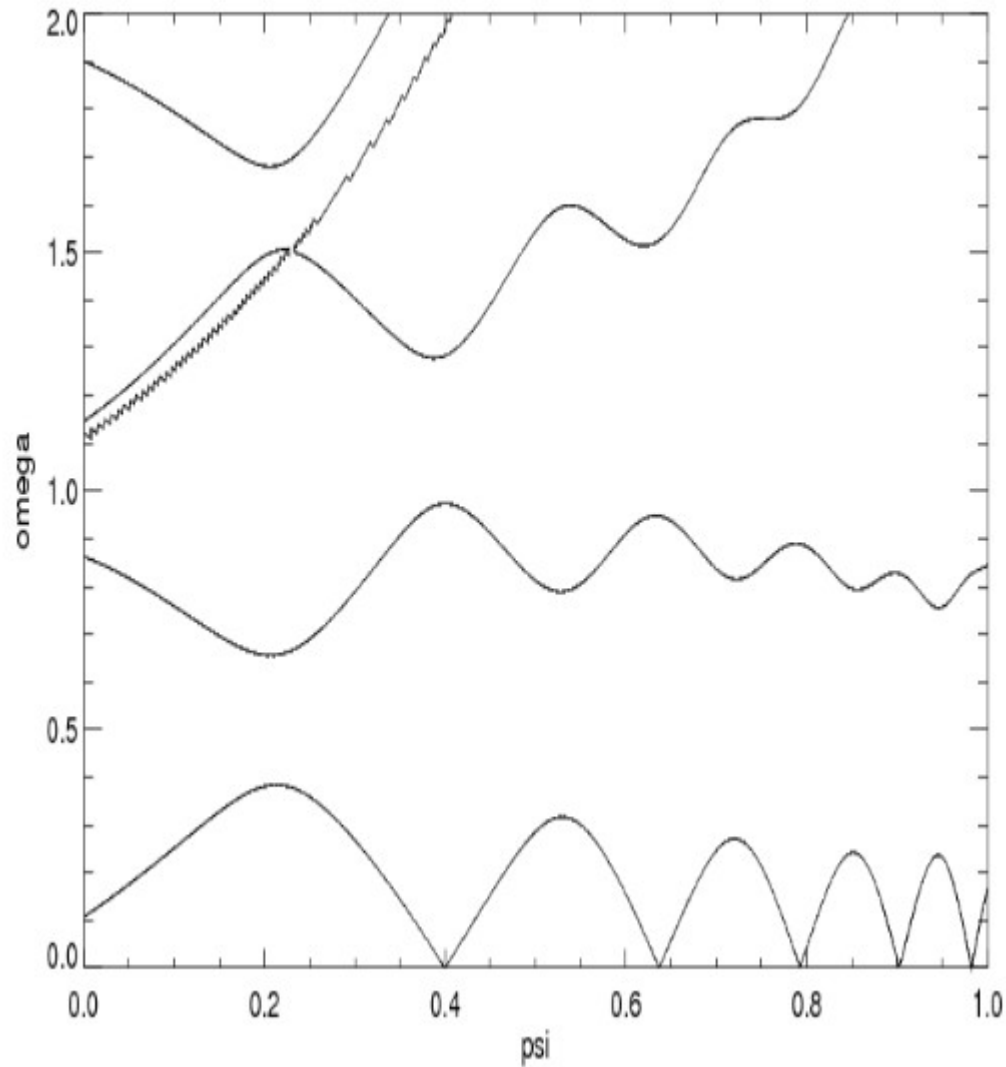
$$+ 2nG_{23}v_3^2 + \mathbf{M}G_{33}v_3^2 + 2iv_1^2G'_{12} + 2iv_1v_2G'_{22} + 2iv_1v_3G'_{23}$$

$$+ 2G_{12}v_1(-\mathbf{M}v_2 + nv_3 + iv'_1) + 2iG_{22}v_1v'_2 + 2iG_{23}v_1v'_3) \nabla \theta$$

$$+ e^{-2in\zeta} (2i\mathbf{M}G_{33}v_2v_3 - inG_{33}v_3^2 + v_1^2G_{13} + v_1v_2G'_{23} + v_1v_3G'_{33}$$

$$+ G_{13}v_1(2i\mathbf{M}v_2 - inv_3 + v'_1) + G_{23}(iv_2(2\mathbf{M}v_2 - nv_3) + v_1v'_2) + G_{33}v_1v'_3) \nabla \zeta$$

# Frequency Gap



# Conclusions

- AEGIS has been upgraded to include source inversion.
- The new subroutine has been checked with driving frequency close to the TAE frequency. The results are consistent with what we expect.
- The code will be applied to the evaluation of 2<sup>nd</sup> harmonics of Alfvén Eigenmodes.